Bonding Effects in Graphite

By G. Moss*

School of Physics, University of Melbourne, Parkville, Victoria, Australia, 3052

The planar bonding in graphite is interpreted in terms of the deformation density approach. The calculated ratio of the 100 and 110 structure factors is in good agreement with experimental results. This suggests possibly a general means of comparing bonding effects in structures where either the strength of the bonding or the atomic environment is similar and where the bonding parameters in one of the structures are known.

Introduction

Goodman (1976) has measured the absolute structure factors of the 100 and 110 reflections in graphite by convergent-beam electron diffraction. These results support the earlier conclusion of Franklin (1950) that the 100 structure factor is larger than that calculated on the basis of the free-atom model. On the other hand, the 110 structure factor was found to be smaller than the free-atom result. Comparison of the experimental values with those calculated using the Dirac–Slater spherical scattering factors of Cromer & Waber (1965) and the relativistic Hartree–Fock spherical scattering factors due to Doyle & Turner (1968), showed that neither model provides an adequate basis for the description of bonded atoms in graphite.

Failures of the spherical-atom approximation have been observed in a large number of structures; perhaps the most noted being the appearance of the forbidden 222 reflection in the diamond structure (Göttlicher & Wölfel, 1959). In some cases (*e.g.* Dawson, 1967*a*,*b*, *c*) deviations from the free-atom scattering factors have been explained by introducing symmetry-allowed deformation functions. In the present work the deformation density is used to explain the observed 100 and 110 structure-factor values. An empirical method is used for estimating the values of the exponents of the deformation terms and the third-order linear parameter is fixed by physical arguments.

The deformation density in graphite

The atomic charge density may be expanded as a series in symmetry allowed functions (Dawson, 1967*a*). The bonding between the planes in graphite is predominantly of the van der Waals type (Lynch & Drickmayer, 1966) hence terms in the charge-density expansion corresponding to interplanar components

have been neglected in the following. Stewart (1972, 1973*a*) has listed tesseral harmonic functions for all point groups; hence, retaining only intraplanar components to third order, leads to the expression

$$\rho(\mathbf{r}) = \overline{\rho(r)} + \delta\rho_{c,0}(r) + \delta\rho_{a,3}(\mathbf{r}) \qquad (1a)$$

where

$$\delta\rho_{c,0}(r) = \frac{b_0 a_0^5 r^2}{24}\left[1 - \frac{a_0^2 r^2}{30}\right]\exp(-a_0 r) \qquad (1b)$$

$$\delta\rho_{a,3}(\mathbf{r}) = \frac{b_3 a_3^6}{120}[uv^2 - u^2 v]\, r^3 \exp(-a_3 r). \qquad (1c)$$

(u,v,w) are hexagonal directional cosines (a_0,b_0) and (a_3,b_3) are respectively the zeroth and third-order bonding parameters and the subscripts c and a refer to the centrosymmetric and antisymmetric nature of the deformation terms. In the above, $\overline{\rho(r)}$ is the prepared spherical atom model, $\delta\rho_{c,0}(r)$ represents a spherical expansion/contraction of the bonded atom relative to $\overline{\rho(r)}$, $\delta\rho_{a,3}(\mathbf{r})$ is the angle-dependent deformation function corresponding to nearest-neighbour bonding within the atomic planes and both deformation terms are normalized to zero to conserve the atomic charge. Fourier transforming equations (1) then yields the atomic scattering factor expansion

$$f(\mathbf{s}) = f(s) + \delta f_{c,0}(s) + i\delta f_{a,3}(\mathbf{s}), \qquad (2a)$$

where $f(s)$ is the free atom spherical scattering factor,

$$\delta f_{c,0}(s) = b_0 \frac{4\pi a_0^6 p^2}{3(a_0^2 + p^2)^6}[13a_0^4 - 6a_0^2 p^2 - 3p^4] \qquad (2b)$$

$$\delta f_{a,3}(\mathbf{s}) = -b_3 H_3 \frac{64\pi a_3^7 p^3}{5(a_3^2 + p^2)^5} \qquad (2c)$$

$$H_3 = \frac{8(k - h)}{27N^3 a_0^3}[2h^2 + 5hk + 2k^2] \qquad (2d)$$

$$p = 2\pi N = 4\pi \sin\theta/\lambda.$$

---

* Present address; Chemical Physics Laboratory, Twente University of Technology, Enschede, The Netherlands.

a_0 is the lattice parameter in the basal plane and hkl are the Miller indices.

The angular function H_3 shows that the 110 structure factor is independent of $\delta f_{a,3}(s)$ and is therefore influenced only by spherical deviations from the free-atom model. The 100 reflection, however, is affected by contributions from both deformation functions.

Parameter estimates

Values of the exponents α_0 and α_3 were estimated from the results of an analysis of the bonding in silicon (Moss, 1977). Dawson (1967a,b,c) has observed that the ratio of the maximum of the third-order deformation function (i.e. the nearest-neighbour contribution to the bonding) to the interatomic distance in diamond, silicon and germanium is approximately constant. A similar scaling of the bonding wavefunctions with lattice parameter has been suggested by Reed & Eisenberger (1972) on the basis of a Compton-profile study of these structures. Extending this concept to the planar bonds in graphite and using a value of 0·4 for the ratio as determined for silicon, leads to the value for α_3 listed in Table 1. The zeroth-order exponent was chosen to give the same value for the ratio α_0/α_3 as found in silicon ($\sim$1·2). As there appears to be very little justification for this choice, a second model was also constructed assuming a ratio of unity.

The 110 structure factor, being independent of $\delta f_{a,3}(s)$ was used to determine b_0, by requiring the experimental and calculated values to be the same.

Phillips (1968) has estimated the bond charge in graphite to be twice that in diamond. Defining the charge redistributed into the bond region to be (cf. Dawson, 1967a)

$$N_{3+} = \int_{\varphi=0}^{\pi/3} \int_{\theta=\pi/4}^{3\pi/4} \int_{r=0}^{\infty} \delta\rho_{a,3}(\mathbf{r}) \, d\mathbf{r} \qquad (3)$$

and assuming this to be twice the corresponding result in diamond (Stewart, 1973b), gave b_3 as listed in Table 1.

Table 1. *Estimated bonding parameters in graphite*

	Model (a)	Model (b)
α_0	6·5	5·6
b_0	−0·03	−0·06
α_3	5·6	5·6
b_3	0·5	0·5

Calculated bonding effects

Three different calculations of the bonding effects in graphite were made. The different models used are designated $d3$, $d03(a)$ and $d03(b)$ and correspond respectively to third-order deformations only, zeroth and third-order deformations using parameters (a) of

Table 2. *Calculated and experimental structure factors*

h k l	Spherical	d3	d03(a)	d03(b)	Experimental*
1 0 0	3·08	3·65	3·55	3·47	3·48 ± 0·05
1 0 1	5·08	5·95	5·79	5·67	
1 1 0	7·40	7·40	7·27	7·27	7·27 ± 0·15
2 0 0	1·66	1·30	1·29	1·29	
2 0 1	2·83	2·26	2·23	2·24	
$\dfrac{\|F(100)\|}{\|F(110)\|}$	0·42	0·49	0·49	0·48	0·48 ± 0·02

* Goodman (1976).

Table 1 and a similar notation for calculations using parameters (b). The relativistic Hartree–Fock (R–HF) model (Doyle & Turner, 1968) was used since this model had previously been employed for the analysis of silicon (Moss, 1977), upon which the estimates of the exponents were based. Anomalous dispersion was neglected and the lattice parameters and thermal
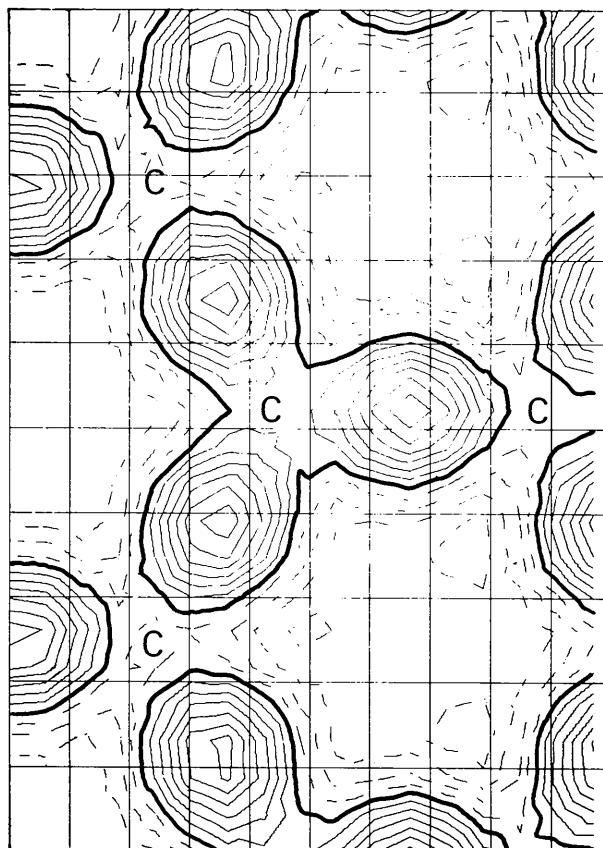

Fig. 1. Calculated Fourier difference map in the basal plane using the difference coefficients $\{F[R\text{–HF}] - F[d03(a)]\}$. Broken lines denote negative contours and the zero level is shown by the heavy line.

parameters of Trucano & Chen (1975) were assumed. The results of these calculations, together with the values of the ratio $|F(100)|/|F(110)|$ are given in Table 2.

It is clear that the R–HF model gives a poor basis for the description of the atomic charge density in graphite. Including only the third-order deformation term improves the agreement between the observed and calculated 100 structure factor values. Including the zeroth-order term further improves the agreement between the experimental and calculated results. The sign of the zeroth-order constant indicates a relaxation of the bonded atom relative to the R–HF model, that is, charge is removed from the region close to the nucleus with a corresponding increase in the vicinity of the valence electrons. A similar effect has also been found in silicon (*e.g.* Aldred & Hart, 1973; Moss, 1977; Price, Maslen & Mair, 1977).

It is not possible, on the basis of the calculated 100 structure factors of Table 2, to differentiate between the two models employed for the zeroth-order bonding parameters. This is also indicated by the similarity of the Fourier difference maps shown in Figs. 1 and 2, calculated from parameters (*a*) and (*b*) respectively. In view of the small interatomic distance within the graphite planes, it is unlikely that different values of the exponents α_0 and α_3 could be reliably detected. Where the separation of nearest neighbours is large, however, differences between models (*a*) and (*b*) become more pronounced and separate exponents become necessary as in the case of silicon.

For all models the values of the 101, 200 and 201 structure factors are significantly different from the spherical-atom values. It would therefore be extremely interesting to measure these reflections and compare them with the predictions listed in Table 2.

Conclusions

The agreement between the calculated and observed ratio of 100 and 110 structure factors is remarkably good, considering the approximate nature of the parameter estimates. The results are encouraging and suggest that this method of estimating the bonding parameters may have more general applicability. Where either the strength of bonding or the atomic environment in two structures is similar it may be possible, by such scaling, to predict the magnitude and nature of bonding in one from the known parameters of the other (*cf.* Bader, Beddell & Peslak, 1973).

Fig. 2. Calculated Fourier difference map in the basal plane using the difference coefficients $\{F[R\text{–HF}] - F[d03(b)]\}$. Contour intervals are the same as in Fig. 1.

References

ALDRED, P. J. E. & HART, M. (1973). *Proc. R. Soc. London*, A**332**, 239–254.

BADER, R. F. W., BEDDALL, P. M. & PESLAK, J. JR (1973). *J. Chem. Phys.* **58**, 557–566.

CROMER, D. T. & WABER, J. T. (1965). *Acta Cryst.* **18**, 104–109.

DAWSON, B. (1967a). *Proc. R. Soc. London*, A**298**, 264–288.

DAWSON, B. (1967b). *Proc. R. Soc. London*, A**298**, 379–394.

DAWSON, B. (1967c). *Proc. R. Soc. London*, A**298**, 395–401.

DOYLE, P. A. & TURNER, P. S. (1968). *Acta Cryst.* A**24**, 390–397.

FRANKLIN, R. E. (1950). *Nature (London)*, **165**, 71–72.

GOODMAN, P. (1976). *Acta Cryst.* A**32**, 793–798.

GÖTTLICHER, S. & WÖLFEL, W. (1959). *Z. Electrochem.* **63**, 891–901.

LYNCH, R. W. & DRICKAMER, H. G. (1966). *J. Chem. Phys.* **44**, 181–184.
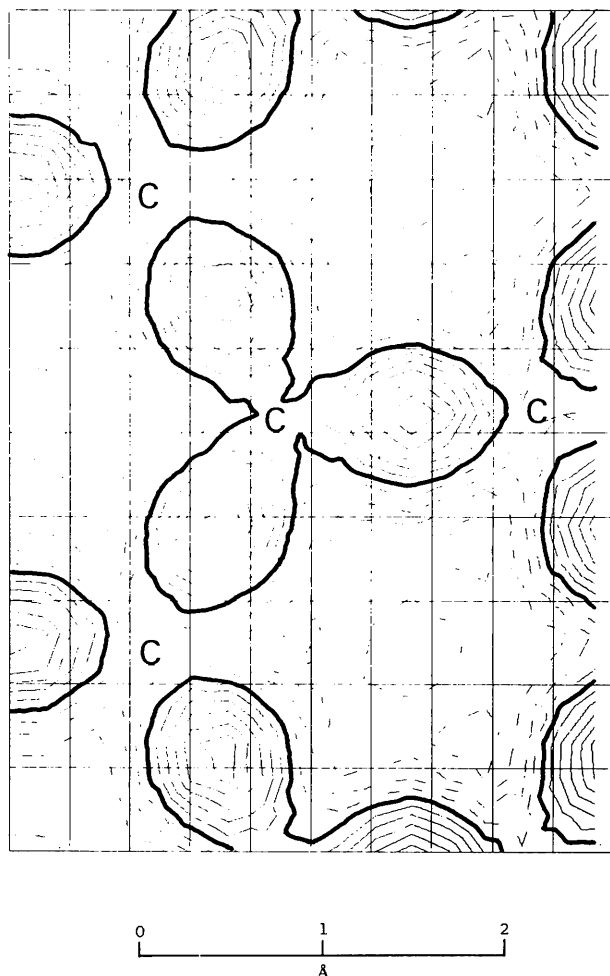
MOSS, G. (1977). PhD Thesis, Univ. of Melbourne.

PHILLIPS, J. C. (1968). *Phys. Rev.* **168**, 912–917.
PRICE, P. F., MASLEN, E. N. & MAIR, S. L. (1977). *Acta Cryst.* A. In the press.
REED, W. A. & EISENBERGER, P. (1972). *Phys. Rev.* **B6**, 4596–4604.

STEWART, R. F. (1972). Unpublished.
STEWART, R. F. (1973a). *J. Chem. Phys.* **58**, 1668–1676.
STEWART, R. F. (1973b). *J. Chem. Phys.* **58**, 4430–4438.
TRUCANO, P. & CHEN, R. (1975). *Nature (London)*, **258**, 136–137.

The Scattering of High-Energy Electrons.
I. Feynman Path-Integral Formulation

BY BING K. JAP AND ROBERT M. GLAESER

Division of Medical Physics and Donner Laboratory, University of California, Berkeley, California 94720, USA

The Feynman path-integral formulation of quantum mechanics is used to investigate the theoretical problem of the propagation of high-energy electrons through thin crystalline specimens. The primary objective is to find a satisfactory scattering approximation that accurately describes the transmitted (elastically scattered) wave, and still retains a mathematically invertible relation between the transmitted wave function and the specimen structure. It is shown that the path-integral method leads naturally to an invertible, higher-order, phase-object approximation, in addition to the usual kinematic approximation and the usual phase-object approximation. The higher-order phase-object approximation in turn leads to the noninvertible, multislice approximation of Cowley & Moodie, which had previously been derived by those authors from a semi-classical, physical-optics point of view.

Introduction

As early as 1928, Bethe developed the dynamical theory of electron diffraction. The theory gives, however, a solution which is highly complicated and also tedious to be applied to cases where more than two diffracted beams are considered. In subsequent years, the problem of dynamical scattering of electrons has been approached by a variety of theoretical methods, including the 'physical-optics' method of Cowley & Moodie (1957), an extension of Bethe's eigenvalue method (*i.e.* the Bloch wave method) by Howie & Whelan (1961), use of the Born series as developed by Fujiwara (1959), and use of the scattering-matrix method as given, for example, by Sturkey (1962) and by Fujimoto (1959). A full quantum-field theoretical method has also been applied (Ohtsuki & Yanagawa, 1966). A comparison of these approaches has recently been discussed in some detail by Goodman & Moodie (1974). Only recently have rigorous attempts been made to use the multislice dynamical theory of Cowley & Moodie (1957) for interpretation of electron images (Allpress, Hewat, Moodie & Sanders, 1972; Lynch, Moodie & O'Keefe, 1975). Up to now the work has been limited to inorganic crystals.

In this paper we present the derivation of four different high-energy electron-scattering approxima-tions, following the Feynman path-integral formulation of quantum mechanics. The four approximations are, in order of increasing complexity, the kinematic approximation, the phase-object approximation, a higher-order phase-object approximation (not pre-viously described) and the multislice approximation of Cowley & Moodie (1957). The conditions under which each of these approximations has a useful degree of validity is explored by representative, numerical calculations in the subsequent papers of the series. It is worth noting that these approximations, except for the multislice formulation, give an invertible relation between the transmitted wave function and the projected object potential. Thus the projected potential can be retrieved from the wave function, which can, in principle, be determined from the image intensities (see for example Misell, Burge & Greenaway, 1974; Lannes, 1976).

The path-integral formulation of quantum mechanics developed by Feynman (1948) and Feynman & Hibbs (1965) appears to be a logical as well as an intuitive way of dealing with the scattering problem for high-energy electrons. The classical limit arises naturally in this formulation as a special case of quantum mechanics, when the quantities such as mass and velocity are so large that Planck's constant can be considered infinitesimal (Feynman & Hibbs, 1965). The path-integral formulation has been shown to be